


Quantum Rabi Oscillations in Coherent and in Mesoscopic Cat Field States

F. Assemat, D. Grosso, A. Signoles, A. Facon, I. Dotsenko, S. Haroche, J. M. Raimond, M. Brune, and S. Gleyzes*
*Laboratoire Kastler Brossel, Collège de France, CNRS, ENS-Université PSL,
 Sorbonne Université, 11, place Marcelin Berthelot, 75005 Paris, France*

 (Received 14 May 2019; published 2 October 2019)

The simple resonant Rabi oscillation of a two-level system in a single-mode coherent field reveals complex features at the mesoscopic scale, with oscillation collapses and revivals. Using slow circular Rydberg atoms interacting with a superconducting microwave cavity, we explore this phenomenon in an unprecedented range of interaction times and photon numbers. We demonstrate the efficient production of cat states, which are the quantum superposition of coherent components with nearly opposite phases and sizes in the range of few tens of photons. We measure cuts of their Wigner functions revealing their quantum coherence and observe their fast decoherence. This experiment opens promising perspectives for the rapid generation and manipulation of nonclassical states in cavity and circuit quantum electrodynamics.

DOI: 10.1103/PhysRevLett.123.143605

The Rabi oscillations of a two-level atom in a resonant, single-mode coherent field state is one of the simplest phenomena in quantum optics. Nevertheless, it exhibits surprisingly complex features at the mesoscopic scale (few tens of photons) [1–4]. The oscillations, at an angular frequency $\Omega_0\sqrt{\bar{n}}$, collapse and revive (\bar{n} is the average photon number in the coherent state; Ω_0 is the vacuum Rabi frequency measuring the atom-field coupling). The collapse, occurring on a timescale $T_c = 2\sqrt{2}/\Omega_0$, results from the quantum field amplitude uncertainty and from the corresponding dephasing of the Rabi oscillations. The (first) revival, around $T_r = 4\pi\sqrt{\bar{n}}/\Omega_0$, results from the rephasing of oscillations associated to different photon numbers [5]. This revival provides a landmark illustration of field amplitude quantization [10]. Between collapse and revival, the field evolves into an entangled atom-field state, involving two coherent states with different phases [11–15]. It is called a cat state in memory of Schrödinger’s metaphor. Close to $t = T_r/2$, the atomic state factors out of a field cat, with the superposition of coherent states with opposite phases [5].

These phenomena can be observed in systems implementing the Jaynes and Cummings model, a spin-1/2 coupled to a one-dimensional harmonic oscillator [16]. Ions in traps [17,18], cavity quantum electrodynamics (CQED) [3,10], and circuit quantum electrodynamics (cQED) [19–21] are thus ideal platforms for this observation.

Experiments on the mechanical oscillation of ions in a trap [17,22] recently observed revivals for phonon numbers around 20 [23]. However, in the important case of a field oscillator, quantum revivals have so far been limited to small photon numbers since experiments face formidable challenges. For microwave CQED with superconducting cavities crossed by fast Rydberg atoms, the interaction time is limited to a few vacuum Rabi periods, $2\pi/\Omega_0$. Revivals

have been observed only for $\bar{n} \simeq 1$ [10,24]. Early revivals induced by a time-reversal of the collapse can be observed for larger \bar{n} values (about 10), but the maximum separation of the cat components is small [25,26]. In cQED, the limited coherence time of tunable superconducting qubits makes it difficult to observe long-term dynamics in the resonant regime [21,27]. Large cat-state preparation so far relies mostly instead on the dispersive, nonresonant interaction [19,28], in which the atom is simply a transparent dielectric material with a state-dependent index of refraction [3].

In this Letter, we push the quantum revival phenomenon at a much larger scale. Using slow circular Rydberg atoms crossing a high- Q superconducting cavity, we achieve atom-field interaction times up to 20 vacuum Rabi oscillations periods. We observe the complete first revival for $\bar{n} = 13.2$. Resetting the atom close to $t = T_r/2$, we leave in the cavity a cat state. We observe the quantum revivals in this initial cat state. We use them to measure the cat state Wigner function and to investigate its fast decoherence.

The experiment is sketched in Fig. 1(a). Additional details are given in the Supplemental Material [5]. A 2D-MOT and an additional longitudinal velocity selection produce a Rubidium atomic beam propagating upwards along the Ox axis at an average velocity $v = 8.1$ m/s towards the cavity C .

Inside the cavity, atomic samples are selectively prepared in $|e\rangle$, the circular state $51c$ with a principal quantum number 51, by laser, radio-frequency, and microwave excitation [29]. Each sample contains 0.08 atoms on the average. Events with two atoms simultaneously present in C have thus negligible influence. The cavity is tuned close to resonance with the $|e\rangle \rightarrow |g\rangle$ transition at 51.1 GHz ($|g\rangle$ is the $50c$ circular state). An electric field along the cavity axis, Oy , produced by a voltage applied across the mirrors, stabilizes the circular states and makes it

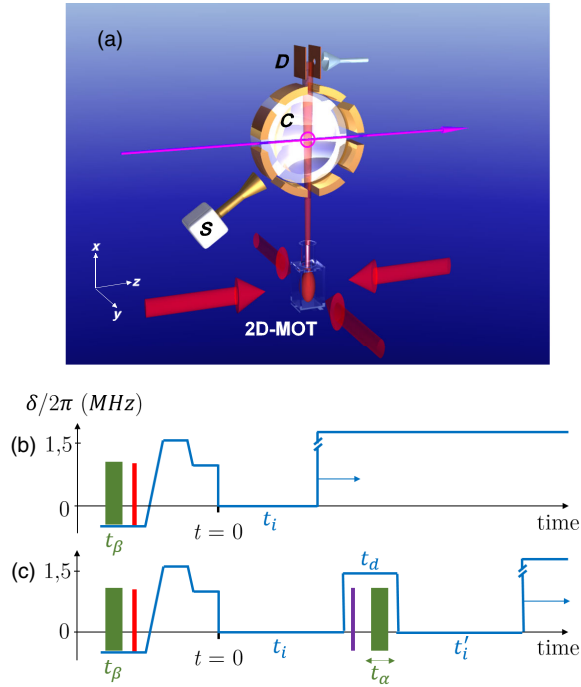


FIG. 1. (a) Sketch of the experimental setup (only one cavity mirror shown for clarity), with the axis conventions. (b) Timing of the Rabi oscillation sequence. The solid blue line depicts the atom-cavity detuning δ as a function of time (timescale is qualitative). The resonant interaction starts at $t = 0$ and lasts for a variable interaction time t_i . The green bar depicts the mw injection in C starting at $t = -71 \mu\text{s}$ and lasting t_β ; the red bar is the exciting laser pulse at $t = -25 \mu\text{s}$. The circular state preparation sequence takes place between the laser pulse and $t = 0$. (c) Timing of the cat revival experiment. Same conventions as for (b). The two resonant interactions last for a fixed time $t_i = 60 \mu\text{s}$ and a variable time t'_i . They are separated by the variable delay t_d during which $|g\rangle$ is eliminated (purple bar) and an injection lasting t_α is performed (green bar).

possible to Stark-tune the atomic transition frequency in or out of resonance with C . After the interaction with the cavity mode, the atoms drift towards a field-ionization counter D , allowing us to measure the populations in $|e\rangle$ or $|g\rangle$ (see the Supplemental Material [5] for details).

The cavity C , cooled down to 1.5 K by a wet ^4He cryostat, sustains a linearly polarized Gaussian standing-wave mode with a waist $w = 6 \text{ mm}$ [3]. Its damping time is $T_{\text{cav}} = 8.1 \pm 0.3 \text{ ms}$. Its temperature corresponds to an average thermal photon number $n_{\text{th}} = 0.38$. In order to reduce the residual photon number in C , we send absorbing atoms prepared in $|g\rangle$, starting 2.7 ms before the sequence. A microwave source S , coupled to C , performs tunable coherent displacements of its mode. The injected amplitude β is a linear function of the injection time t_β . For injections lasting more than $\approx 100 \text{ ns}$, the calibration is $|\beta| = 0.26t_\beta(\mu\text{s}) - 0.05$ [5].

We first record the vacuum Rabi oscillations with no injection ($\beta = 0$) and an atom initially in $|e\rangle$. The sequence

timing is sketched in Fig. 1(b). The initial state $|e\rangle$ is prepared in a large electric field, resulting in a $\delta/2\pi = 1.4 \text{ MHz}$ atom-cavity detuning, for which the interaction is negligible. We abruptly set $\delta = 0$ at $t = 0$. After a variable interaction time t_i , we set back δ to a large value ($2\pi \times 4.04 \text{ MHz}$), halting the evolution. We measure the probability, P_g , for finding the atom in $|g\rangle$.

Figure 2(a) shows the experimental $P_g(t_e)$ (dots with statistical error bars, joined by a thin black line) as a

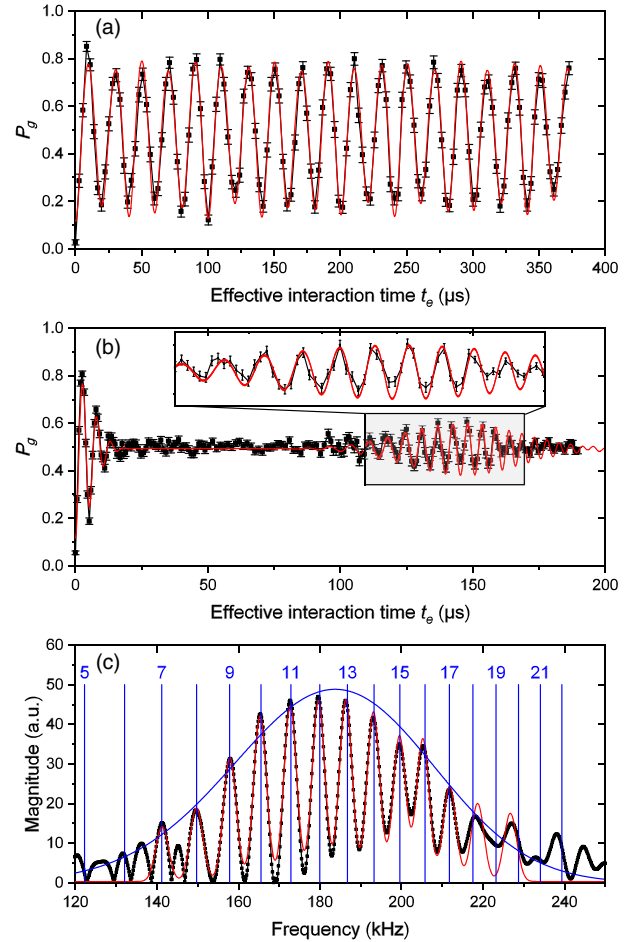


FIG. 2. (a) Vacuum Rabi oscillation. Dots with statistical error bars joined by a thin black line: experimental probability $P_g(t_e)$ as a function of the effective interaction time t_e . Solid red line: numerical simulation of the experiment. (b) Rabi revival in a 13.2-photon initial coherent field. Dots with statistical error bars joined by a thin black line: experimental probability $P_g(t_e)$. Solid red line: numerical simulation of the experiment. The inset shows an enlargement of the revival. (c) Fourier transform of the signal in (b) (black dots). The solid red line is a fit to a superposition of Gaussian peaks. The vertical dotted blue lines are at the expected Rabi frequencies for photon numbers, n , given on top. The blue solid line is the envelope of the Poisson photon number distribution for a 13 photon coherent state (corresponding to an initial 13.2 photons field when taking into account cavity relaxation), adjusted in height to fit the arbitrary scale of the Fourier Transform.

function of the effective interaction time t_e taking into account the motion of the atom through the Gaussian mode geometry [5]. We observe nearly 20 vacuum Rabi periods, a considerable improvement over previous experiments [10]. The red line in Fig. 2(a) results from a numerical simulation of the experiment taking into account the detection imperfections, resulting in a reduced oscillation contrast, as well as the residual initial thermal field and cavity relaxation towards thermal equilibrium [5]. The precise value of the Rabi frequency is extracted from a fitting procedure described in the Supplemental Material [5]. It is found to be $\Omega_0/2\pi = 49.8$ kHz, very close to the value deduced from the atom and cavity characteristics (50 kHz). The probability $p_1 = 0.09$ for having initially one photon in C and the precise position of the exciting laser beams inside the cavity mode, defining the relation between the real and effective interaction times, are also extracted from this fit.

We record now the Rabi oscillation in a coherent state $|\beta\rangle$ [timing in Fig. 1(b), with $t_\beta = 14 \mu\text{s}$]. Note that β can be assumed to be real without loss of generality. The signal is plotted in Fig. 2(b) (points with statistical error bars joined by a thin black line). It clearly exhibits the first revival around $T_r = 146 \mu\text{s}$. The Fourier transform of the revival signal [dots in Fig. 2(c) with a fit to a sum of Gaussians—solid red line] exhibits discrete peaks, very close to the expected Rabi frequencies in an n -photon field, $\Omega_0\sqrt{n+1}/2\pi$ (vertical blue lines). They are well-resolved up to about 18 photons. This signal provides textbook evidence of field quantization.

The weight of the peaks directly measures the photon number distribution, $p(n)$ [5]. It is in excellent agreement with a Poisson distribution for a mean photon number 13.0 (blue solid line). Taking into account cavity relaxation, this corresponds to a 13.2 photon initial field, in excellent agreement with the injection calibration. The red solid line in Fig. 2(b) is a numerical simulation of the experiment using this initial photon number. It takes into account the same imperfections as those in Fig. 2(a). It is in excellent agreement with the experimental data.

Close to half the revival time, $t_e \approx T_r/2 \approx 73 \mu\text{s}$, the atomic state is expected to factor out [5]. The cavity is then in a superposition of two components with nearly opposite phases [12,13]. The field Wigner function, $W(\alpha)$, exhibits fringes near the origin of phase space revealing the cat's coherence [30]. It has been shown that this cat's parity, $\mathcal{P} = \sum_n (-1)^n p(n)$, oscillates with t_e [31].

In order to probe the cavity state, we make use of its resonant interaction with a “probe” atom, initially in $|e\rangle$. For a well-chosen [5] effective interaction time t_e close to $T_r/2$, the probability P_g for finding the atom in $|g\rangle$ is $P_g(t_e) \approx (1 - \mathcal{P})/2$, and P_g measures the parity $\mathcal{P} = \pi W(0)/2$ [23]. By displacing the cat state by α before the resonant interaction, we get access to $W(-\alpha)$.

The timing of the experiment is depicted in Fig. 1(c). We set the first resonant effective interaction time to $t_i = 60 \mu\text{s}$.

After the atom has been tuned out of resonance, we perform a displacement by a real amplitude α (injection time t_a). Simultaneously, we get rid of the $|g\rangle$ part of the atomic state by a resonant radio-frequency pulse transferring $|g\rangle$ to low-magnetic-quantum-number states, finally undetected. Thus, any detected atom was in $|e\rangle$ at the beginning of a new resonant interaction, starting after a delay $t_d = 6 \mu\text{s}$ and lasting for a variable time t'_i corresponding to the effective time t'_e .

Figure 3(a) shows $P_g(t'_e, \alpha)$ (dots with statistical error bars) as a function of α for $t'_e = 67 \mu\text{s} \approx T_r/2$. We have chosen this t'_e value to optimize the contrast of the oscillations, so that $P_g(t'_e, \alpha) \approx [1 - \pi W(-\alpha)/2]/2$.

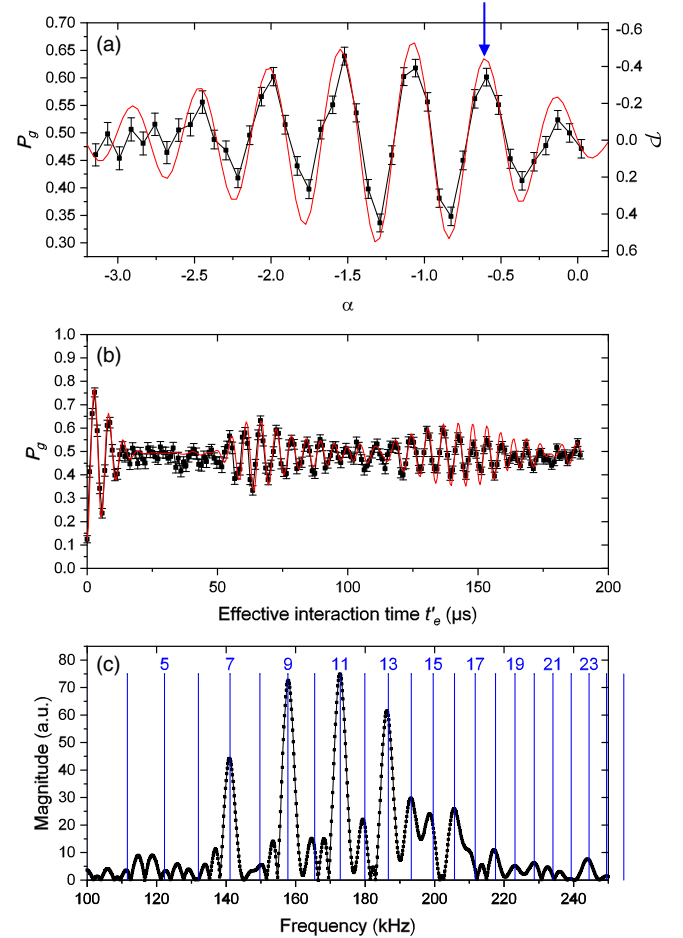


FIG. 3. (a) Measurement of the displaced cat's parity proportional to its Wigner function. $P_g(t'_e, \alpha)$ as a function of α for $t'_e = 68.5 \mu\text{s}$ (dots with statistical error bars joined by a thin solid black line). The solid red line results from a numerical simulation. (b) Quantum revivals in a displaced cat state. $P_g(t'_e, \alpha)$ as a function of t'_e for $\alpha = -0.60$ (dots with statistical error bars and a connecting thin solid black line). The solid red line results from a numerical simulation. The additional revival around $T_r/2$ is clearly visible. (c) Fourier transform of the signal in (b) (dots with connecting thin black line). Vertical blue lines depict the expected Rabi frequencies. The absence of even photon numbers in the distribution is conspicuous.

The solid red line results from the simulation of the experiment and is in excellent agreement with the data. From the period of the oscillations in Fig. 3(a), we deduce the size of the cat, D^2 , measured by the square of the distance D of the superposed components in phase space [5]. We get $D^2 = 45.1 \pm 0.4$ photons in excellent agreement with the value provided by the numerical simulation. This size compares with that of the largest cats ever prepared by dispersive interaction [19].

Figure 3(b) shows $P_g(t'_e, \alpha)$ as a function of the effective interaction time t'_e for $\alpha = -0.60$. This displacement [arrow on Fig. 3(a)] brings one of the extrema of W onto the origin of phase space, resulting in a displaced cat with a maximum parity. We clearly observe here a dual revival, one at the standard revival time T_r and one earlier, at $T_r/2$, revealing the displaced cat parity. The agreement of the experimental data with the simulation (red solid line) is excellent.

The Fourier transform of the Rabi signal, shown in Fig. 3(c), conspicuously displays the displaced cat parity. The photon number distribution inferred from this spectrum provides a displaced cat parity $\mathcal{P} = -0.48$. The simulation provides $\mathcal{P} = -0.41$ in excellent agreement with the observed value. The parity for an ideal experiment, taking into account cavity relaxation, is expected to be -0.49 , very close to the observed one. We thus generate large cats with a good fidelity.

The decoherence time scale of the cat in the finite temperature environment of the cavity is expected to be $200 \mu\text{s}$ [5,32]. In order to investigate this fast decoherence, we monitor the amplitude of the revival at $T_r/2$ as a function of the delay time t_d (note that the displacement by α does not change the dynamics of decoherence).

Figures 4(a)–4(d) show four Rabi oscillations signals for t'_e close to $T_r/2$ for $\alpha = -0.60$ and for four values of t_d (dots with statistical error bars and simulation of the experiment as a solid red line). The agreement between simulation and data is excellent, confirming the decoherence timescale.

In conclusion, we have observed the resonant Rabi oscillation in a coherent field in an unprecedented range of photon numbers. We have shown the generation of large cat states through the first observation of an early revival for the Rabi oscillation in a cat with a well-defined parity. We have monitored the fast decoherence of these nonclassical states.

The resonant interaction generates cat states efficiently and significantly faster than the dispersive method [5]. Using more than one atom, it can lead to the preparation of more complex state superpositions with multiple components [33,34]. It is thus a promising method for fundamental decoherence studies, but also, in the cQED context, for the use of cats in quantum error correction protocols [35,36].

This experiment also opens the way to a new realm for atomic physics CQED, with extremely long interaction

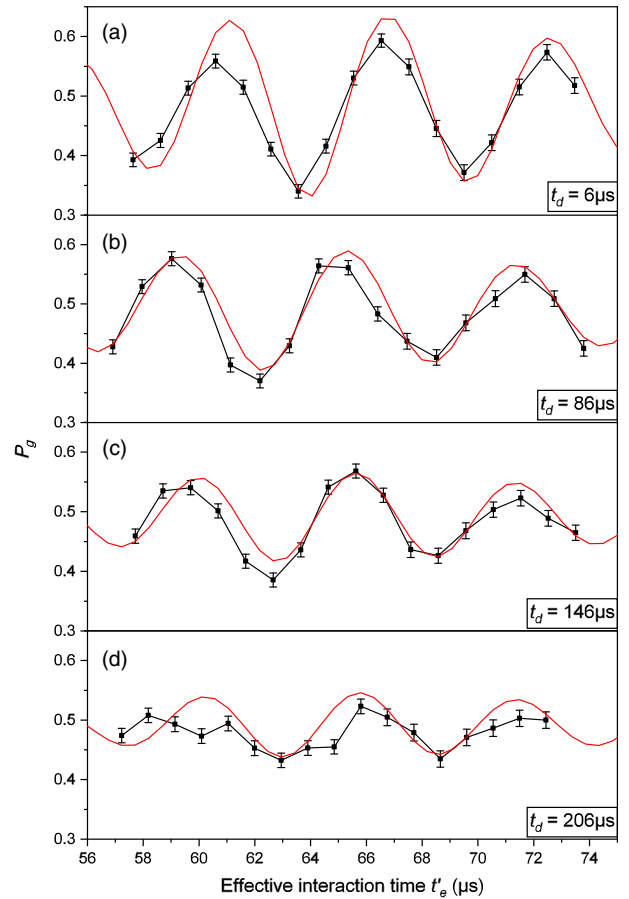


FIG. 4. (a)–(d) Rabi oscillations signals around $T_r/2$ for the probe atom in a displaced cat state for $\alpha = -0.60$ and four delay times $t_d = 6, 86, 146,$ and $206 \mu\text{s}$. Dots with statistical error bars and connecting thin line are the experimental data. The solid red line results from the simulation of the experiment. The fast decrease of the oscillation contrast reveals the cat decoherence.

times and extremely low damping cavities. Particularly promising is the use of laser-trapped circular Rydberg atoms [37]. They could be combined with a 3D-microwave structure sustaining a high-quality resonant mode, but admitting no other modes resonant with the atomic spontaneous emission decay channels. One might then combine the best of the CQED and cQED worlds, with reproducible atoms, well-controlled and understood decoherence channels, nearly infinite interaction times, and the slow pace of CQED experiments instrumental for real-time control [38].

We acknowledge funding by the EU under the ERC projet “DECLIC” (Project No. 246932) and the Research and Innovation Action (RIA) project “RYSQ” (Project No. 640378).

*gleyzes@lkb.ens.fr

[1] J. H. Eberly, N. B. Narozhny, and J. J. Sanchez-Mondragon, *Phys. Rev. Lett.* **44**, 1323 (1980).

- [2] M. Fleischhauer and W. P. Schleich, *Phys. Rev. A* **47**, 4258 (1993).
- [3] J.-M. Raimond, M. Brune, and S. Haroche, *Rev. Mod. Phys.* **73**, 565 (2001).
- [4] I. Feranchuk and A. Leonov, *Phys. Lett. A* **373**, 517 (2009).
- [5] See Supplemental Material at <http://link.aps.org/supplemental/10.1103/PhysRevLett.123.143605> for details about the theoretical model, the experimental apparatus and the data analysis, which includes Refs. [6–9].
- [6] S. Haroche and J.-M. Raimond, *Exploring the Quantum: Atoms, Cavities and Photons* (Oxford University Press, Oxford, 2006).
- [7] L. G. Lutterbach and L. Davidovich, *Phys. Rev. Lett.* **78**, 2547 (1997).
- [8] S. Kuhr, S. Gleyzes, C. Guerlin, J. Bernu, U. B. Hoff, S. Deléglise, S. Osnaghi, M. Brune, J.-M. Raimond, S. Haroche *et al.*, *Appl. Phys. Lett.* **90**, 164101 (2007).
- [9] J. R. Johansson, P. D. Nation, and F. Nori, *Comput. Phys. Commun.* **184**, 1234 (2013).
- [10] M. Brune, F. Schmidt-Kaler, A. Maali, J. Dreyer, E. Hagley, J.-M. Raimond, and S. Haroche, *Phys. Rev. Lett.* **76**, 1800 (1996).
- [11] J. Eiselt and H. Risken, *Opt. Commun.* **72**, 351 (1989).
- [12] J. Gea-Banacloche, *Phys. Rev. Lett.* **65**, 3385 (1990).
- [13] J. Gea-Banacloche, *Phys. Rev. A* **44**, 5913 (1991).
- [14] V. Buzek, H. Moya-Cessa, P. L. Knight, and S. J. D. Phoenix, *Phys. Rev. A* **45**, 8190 (1992).
- [15] I. S. Averbukh, *Phys. Rev. A* **46**, R2205 (1992).
- [16] E. T. Jaynes and F. W. Cummings, *Proc. IEEE* **51**, 89 (1963).
- [17] D. M. Meekhof, C. Monroe, B. E. King, W. M. Itano, and D. J. Wineland, *Phys. Rev. Lett.* **76**, 1796 (1996).
- [18] D. J. Wineland, *Rev. Mod. Phys.* **85**, 1103 (2013).
- [19] B. Vlastakis, G. Kirchmair, Z. Leghtas, S. E. Nigg, L. Frunzio, S. M. Girvin, M. Mirrahimi, M. H. Devoret, and R. J. Schoelkopf, *Science* **342**, 607 (2013).
- [20] C. Wang, Y. Y. Gao, P. Reinhold, R. W. Heeres, N. Ofek, K. Chou, C. Axline, M. Reagor, J. Blumoff, K. M. Sliwa *et al.*, *Science* **352**, 1087 (2016).
- [21] M. Hofheinz, E. M. Weig, M. Ansmann, R. C. Bialczak, E. Lucero, M. Neeley, A. D. O’Connell, H. Wang, J. M. Martinis, and A. N. Cleland, *Nature (London)* **454**, 310 (2008).
- [22] D. Lv, S. An, M. Um, J. Zhang, J.-N. Zhang, M. S. Kim, and K. Kim, *Phys. Rev. A* **95**, 043813 (2017).
- [23] D. Kienzler, C. Flühmann, V. Negnevitsky, H.-Y. Lo, M. Marinelli, D. Nadlinger, and J. P. Home, *Phys. Rev. Lett.* **116**, 140402 (2016).
- [24] G. Rempe, H. Walther, and N. Klein, *Phys. Rev. Lett.* **58**, 353 (1987).
- [25] A. Auffèves, P. Maioli, T. Meunier, S. Gleyzes, G. Nogues, M. Brune, J.-M. Raimond, and S. Haroche, *Phys. Rev. Lett.* **91**, 230405 (2003).
- [26] T. Meunier, S. Gleyzes, P. Maioli, A. Auffèves, G. Nogues, M. Brune, J.-M. Raimond, and S. Haroche, *Phys. Rev. Lett.* **94**, 010401 (2005).
- [27] J. Johansson, S. Saito, T. Meno, H. Nakano, M. Ueda, K. Semba, and H. Takayanagi, *Phys. Rev. Lett.* **96**, (2006).
- [28] G. Kirchmair, B. Vlastakis, Z. Leghtas, S. E. Nigg, H. Paik, E. Ginossar, M. Mirrahimi, L. Frunzio, S. M. Girvin, and R. J. Schoelkopf, *Nature (London)* **495**, 205 (2013).
- [29] A. Signoles, E. K. Dietsche, A. Facon, D. Grosso, S. Haroche, J. M. Raimond, M. Brune, and S. Gleyzes, *Phys. Rev. Lett.* **118**, 253603 (2017).
- [30] S. Deléglise, I. Dotsenko, C. Sayrin, J. Bernu, M. Brune, J.-M. Raimond, and S. Haroche, *Nature (London)* **455**, 510 (2008).
- [31] R. Birrittella, K. Cheng, and C. C. Gerry, *Opt. Commun.* **354**, 286 (2015).
- [32] M. S. Kim and V. Buzek, *Phys. Rev. A* **46**, 4239 (1992).
- [33] P. K. Pathak and G. S. Agarwal, *Phys. Rev. A* **71**, (2005).
- [34] T. Meunier, A. L. Diffon, C. Rueff, P. Degiovanni, and J.-M. Raimond, *Phys. Rev. A* **74**, 033802 (2006).
- [35] N. Ofek, A. Petrenko, R. Heeres, P. Reinhold, Z. Leghtas, B. Vlastakis, Y. Liu, L. Frunzio, S. M. Girvin, L. Jiang *et al.*, *Nature (London)* **536**, 441 (2016).
- [36] S. Rosenblum, P. Reinhold, M. Mirrahimi, L. Jiang, L. Frunzio, and R. J. Schoelkopf, *Science* **361**, 266 (2018).
- [37] T. L. Nguyen, J. M. Raimond, C. Sayrin, R. Cortiñas, T. Cantat-Moltrecht, F. Assemat, I. Dotsenko, S. Gleyzes, S. Haroche, G. Roux *et al.*, *Phys. Rev. X* **8**, 011032 (2018).
- [38] C. Sayrin, I. Dotsenko, X. Zhou, B. Peaudecerf, T. Rybarczyk, S. Gleyzes, P. Rouchon, M. Mirrahimi, H. Amini, M. Brune *et al.*, *Nature (London)* **477**, 73 (2011).